Supplemental material JCB

Chen et al., http://www.jcb.org/cgi/content/full/jcb.201104114/DC1

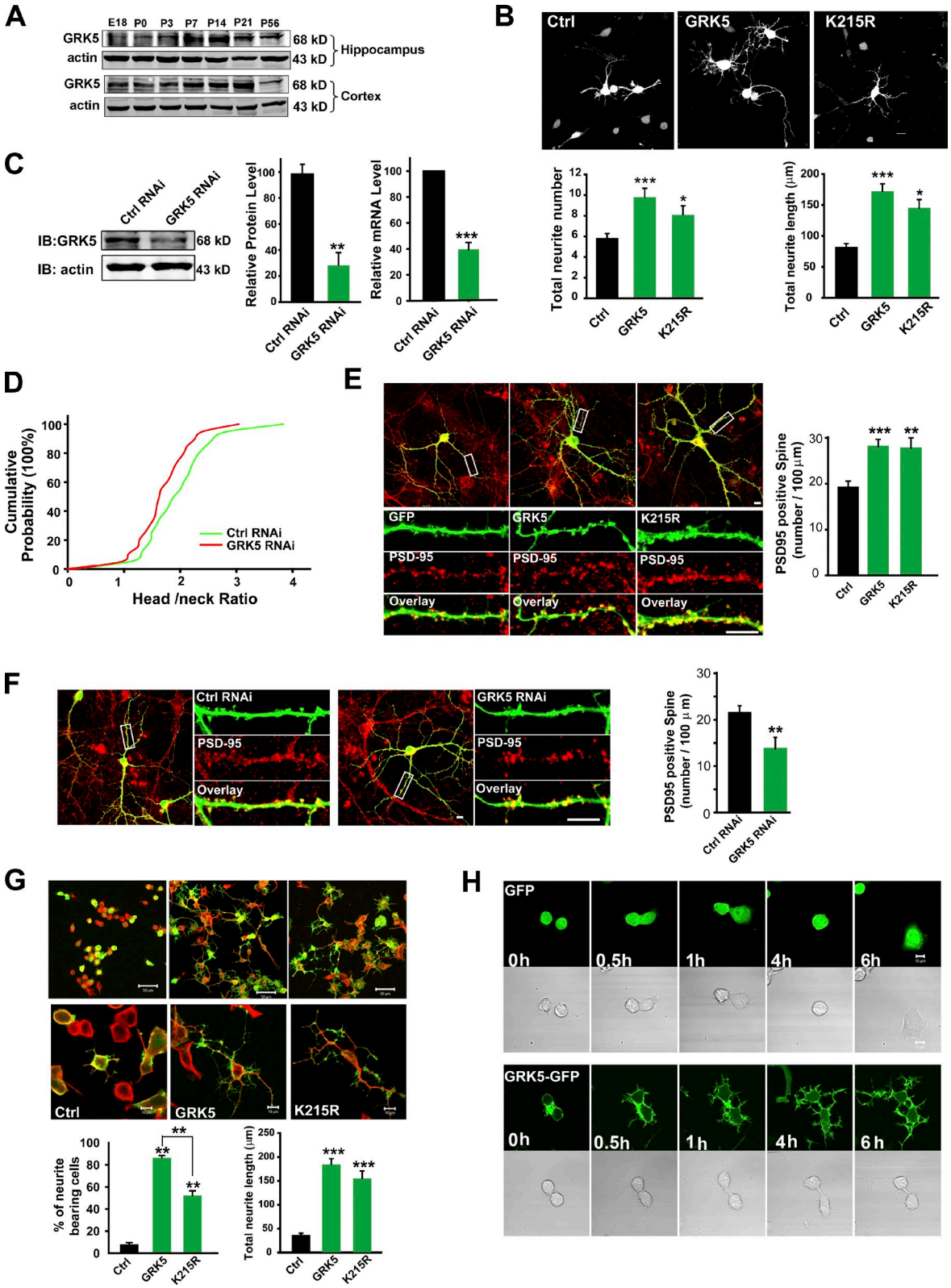

Figure S1. **GRK5 regulates neuritogenesis and dendritic development.** (A) The levels of GRK5 in developing rat hippocampus and cortex were analyzed by Western blotting with GRK5 antibodies. (B) Rat hippocampal neurons were transfected with the indicated plasmids by electroporation after dissection. 24 h later, the number and total length of neurites of 30–40 stage 2 neurons from three independent cultures were analyzed. One-way ANOVA followed by Turkey–Kramer posthoc test. (C) Rat C6 glial cells were transfected with control RNAi or RNAi specifically targeted to rat GRK5. The samples were analyzed by Western blotting and RT-PCR from three independent experiments. Student's *t* test. (D) Distributions of head/neck ratio from the neurons transfected with control RNAi and GRK5 RNAi. 100–150 spines were quantified and analyzed by Kolmogorov-Smirnov test. Head/neck ratio of GRK5 RNAi versus control RNAi: 1.6305 ± 0.4816 μm versus 1.8955 ± 0.5654; $P < 0.05$. (E and F) Hippocampal neurons were transfected at DIV9 and observed at DIV17. Boxed regions are enlarged. For each group, 20–30 dendrites of 8–10 neurons from three independent cultures were analyzed. PSD-95–positive spines were quantified. (E) Neuron cultures were transfected with GFP or HA-tagged GRK5 constructs. One-way ANOVA followed by Turkey–Kramer posthoc test. (F) Neuron cultures transfected with control or GRK5 RNAi constructs. Student's *t* test. (G) Neuro-2a cells transfected with GFP or indicated HA-tagged GRK5 constructs were stained with antibodies against β-tubulin (red) and HA tag (green). The representative cells are given at the bottom. 500–600 cells were analyzed, and the percentages of cells bearing neuritelike processes are plotted. One-way ANOVA followed by Turkey–Kramer posthoc test. (H) Time-lapse imaging of Neuro-2a cells 8 h after transfection with GFP or GRK5-GFP. Error bars indicate SEM. *, $P < 0.05$; **, $P < 0.01$; ***, $P < 0.001$. Ctrl, control. IB, immunoblot. Bars: (A, E–G, bottom, and H) 10 μm; (G, top) 50 μm.

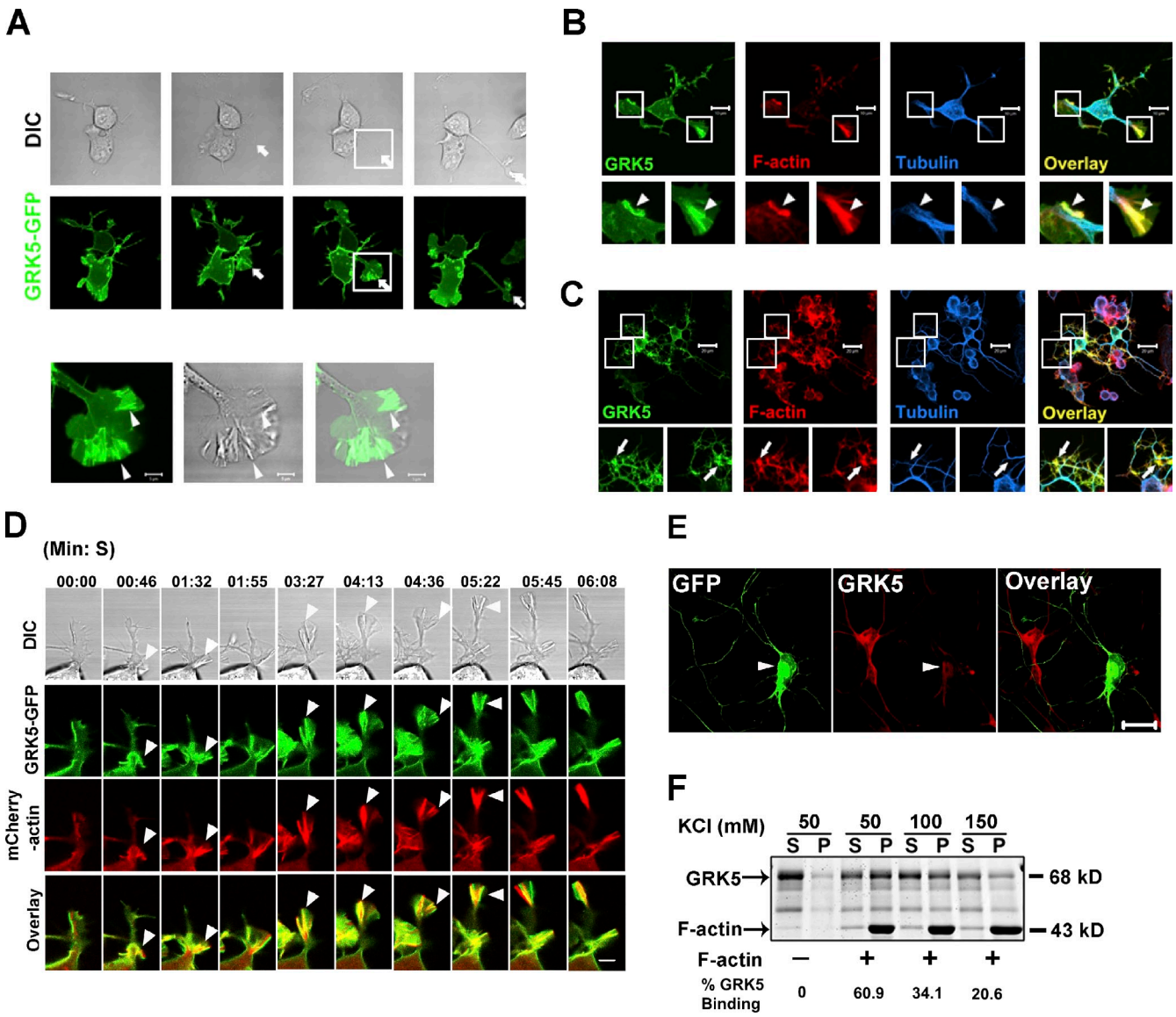

Figure S2. **GRK5 is colocalized with F-actin at sites of actin high dynamic structures.** (A) Time-lapse analysis of living Neuro-2a cells expressing GRK5-GFP. Boxed regions are enlarged below. Arrows indicate the distribution of GRK5 in the growth cone. (B) Colocalization of GRK5 and F-actin in the growth cone of neurites. 9 h after transfection with HA-tagged GRK5, Neuro-2a cells were fixed and stained with a HA-specific antibody (green), antitubulin antibody (blue), or Alexa Fluor 546 phalloidin (red). High-magnification views of growth cone structure enclosed by rectangles are shown below. Arrowheads indicate colocalization of GRK5 with F-actin but not tubulin in the growth cone. (C) Colocalization of GRK5 and F-actin in Neuro-2a cells 24 h after transfection with HA-tagged GRK5. Arrows indicate the colocalization of GRK5 with F-actin but not tubulin at the periphery of cells. (D) Time-lapse analysis of Neuro-2a cells expressing GRK5-GFP (green) and mCherry-actin (red). Differential interference contrast (DIC) shows the morphology of the growing neurite. Arrowheads indicate the colocalization of actin and GRK5 in the tip of a growing neurite. (E) Rat hippocampal neurons were transfected with rat GRK5-RNAi and stained with GRK5 antibodies (G-2) 72 h later. Arrowheads indicate GRK5-RNAi–transfected GFP-positive cells. (F) High-speed sedimentation F-actin–binding assay. 1 μM purified GRK5 was incubated with 2.5 μM F-actin for 30 min in the presence of increasing concentrations of KCl. The percentages of GRK5 bound to F-actin were quantified as the percentage recovered in the pellet subtracted by that recovered in the pellet without F-actin. S, supernatant; P, pellet. Bars: (A and D) 5 μm; (B and E) 10 μm; (C) 20 μm.

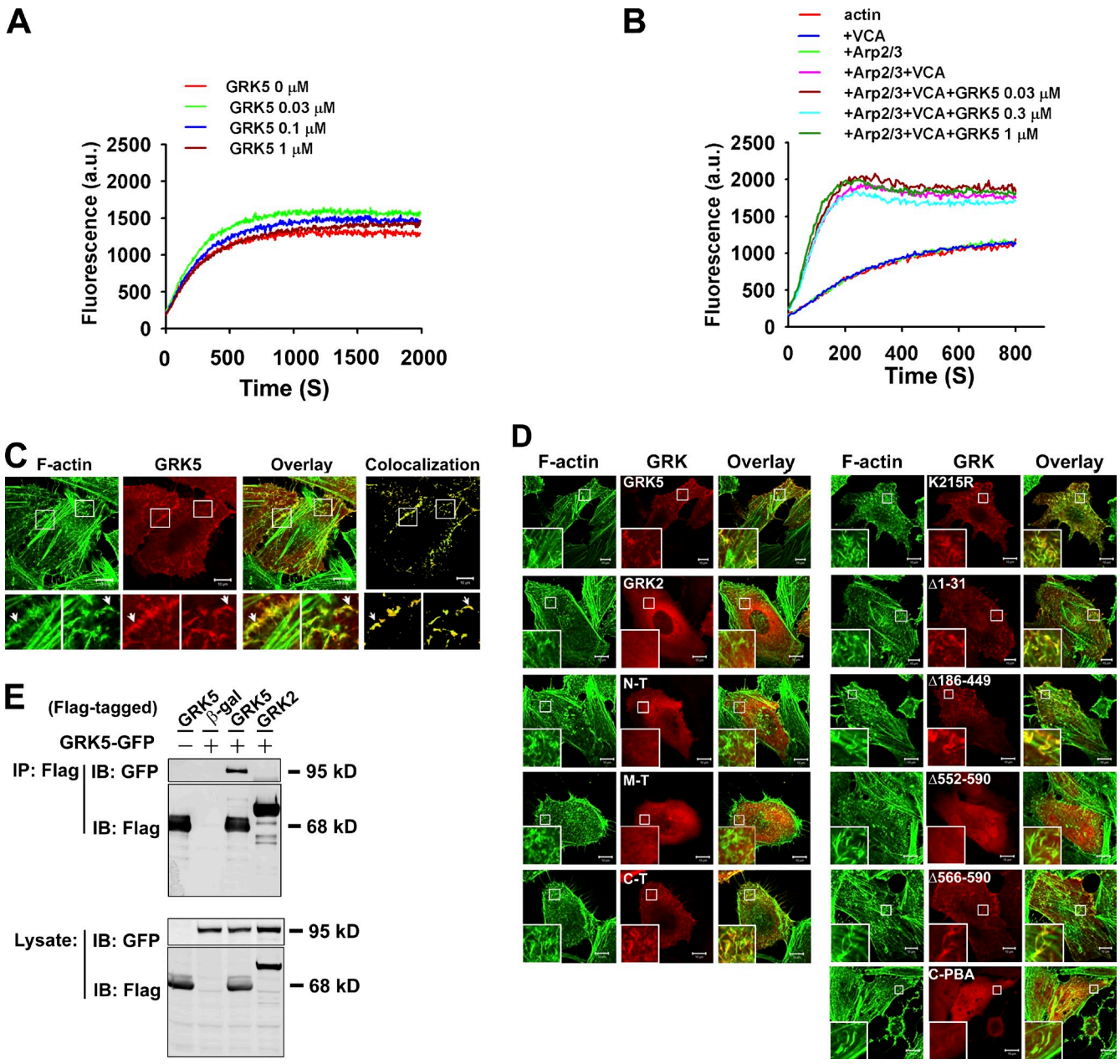

Figure S3. **C-terminal basic residues of GRK5 are essential for its binding to F-actin and self-interaction of GRK5.** (A and B) In vitro polymerization of 2 μM pyrene-labeled actin in the presence or absence of GRK5, VCA, or Arp2/3 was monitored using a fluorescence spectrometer at 5-s intervals. (A) Effect of various concentrations of GRK5. (B) Effect of various concentrations of GRK5 in the presence of VCA and Arp2/3. (C) Colocalization of GRK5 with F-actin in HeLa cells. Cells were transfected with HA-tagged GRK5 and stained with Alexa Fluor 488 phalloidin and the HA antibody. Boxed regions are enlarged below each image. Arrows indicate colocalization of GRK5 with filopodia-like actin filament. (D) HeLa cells transfected with indicated HA-tagged or Flag-tagged GRK variants were stained with Alexa Fluor 488 phalloidin and antibodies against the HA or Flag tag. N-T, M-T, and C-T represent GRK5 truncation mutants containing residues 1–193, 193–431, and 431–590, respectively. Δ1–31, Δ186–449, Δ552–590, and Δ566–590 represent GRK5 deletion mutants lacking the corresponding residues. High-magnification views enclosed by rectangles are shown as insets. (E) HEK293T cells were cotransfected with indicated β-galactosidase (β-gal) or Flag-tagged GRK variants with or without GRK5-GFP. Cell lysates were immunoprecipitated (IP) with M2 beads. The immunocomplexes and the input cell lysates were analyzed by SDS-PAGE and immunoblotting (IB). a.u., arbitrary unit. Bars, 10 μM.

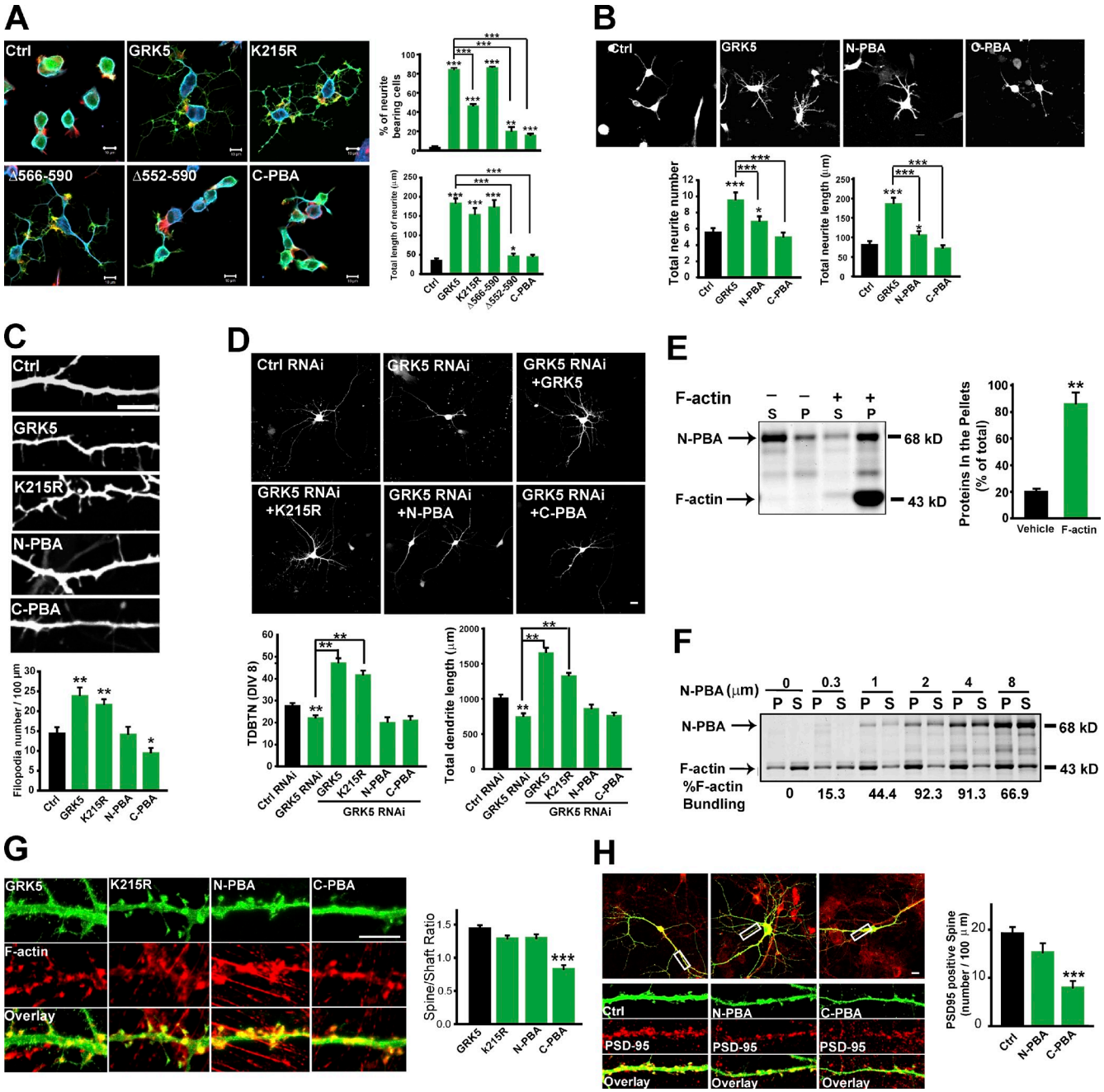

Figure S4. **C-terminal and N-terminal basic residues of GRK5 are critical for its effect on filopodia dynamics and dendritic development.** (A) Neuro-2a cells transfected with GFP or HA-tagged GRK5 variants were stained with a HA-specific antibody (green), anti–β-tubulin antibody (blue), and Alexa Fluor 546 phalloidin (red). The percentages of cells bearing neuritelike processes and total length of neurites were calculated (600 cells analyzed). One-way ANOVA followed by Turkey–Kramer posthoc test. (B) Rat hippocampal neurons were transfected with the indicated plasmids by electroporation after dissection. 24 h later, the number and total length of neurite of 30–40 stage 2 neurons from three independent cultures were analyzed. One-way ANOVA followed by Turkey–Kramer posthoc test). (C) Selected neuritic regions from DIV2 neurons cotransfected with GFP and GRK5 variants are shown. Protrusion density of 20–30 neurons from three independent cultures was measured. (D) Hippocampal neuron cultures were transfected with the indicated constructs on DIV5, and GFP-positive neurons were observed at DIV8. Values of 30–40 neurons from three independent cultures were analyzed. One-way ANOVA followed by Turkey–Kramer posthoc test. (E) High-speed sedimentation F-actin–binding assay. The percentages of proteins bound to F-actin were calculated as the percentage recovered in the pellet. Student's *t* test. (F) Low-speed sedimentation F-actin–bundling assay. The percentage of F-actin present in the bundles was calculated as the percentage of F-actin recovered in the pellet subtracted by that recovered in the pellet without N-PBA. (G) Hippocampal neuron cultures were transfected at DIV9 with HA-tagged GRK5 variants and fixed at DIV17. Cells were stained with a HA-specific antibody and Alexa Fluor 546 phalloidin, and the ratio of staining intensity in spine/shaft was plotted. (H) Hippocampal neurons were transfected with GFP or HA-tagged GRK5 variants at DIV9 and observed at DIV15. PSD-95–positive spines were quantified. For each group, 20–30 dendrites of 8–10 neurons from three independent cultures were analyzed. Boxed regions are enlarged bellow. One-way ANOVA followed by Turkey–Kramer posthoc test. Error bars indicate SEM. *, $P < 0.05$; **, $P < 0.01$; ***, $P < 0.001$. Ctrl, control. Bars, 10 μm.

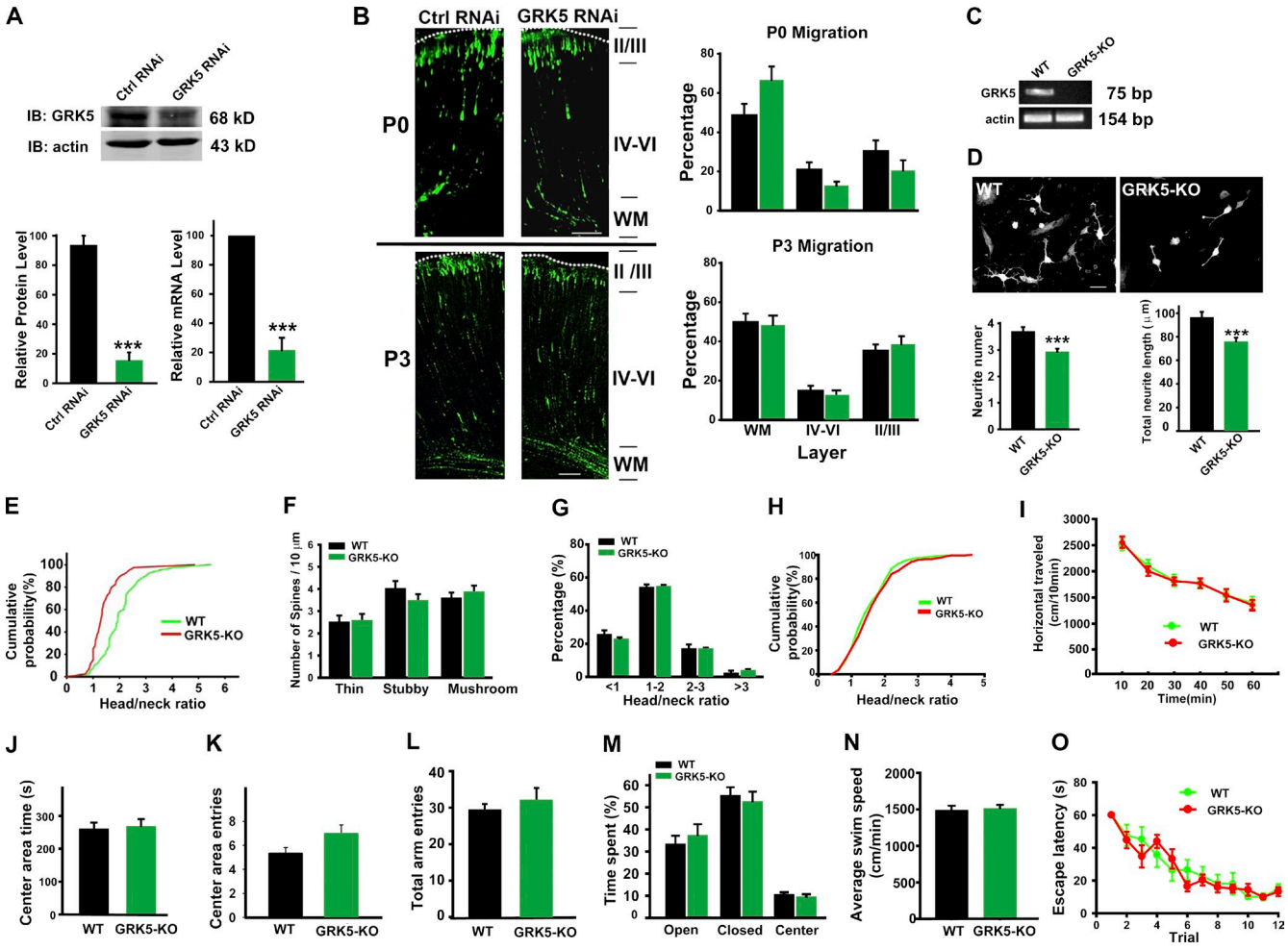

Figure S5. **The effects of depletion of GRK5 in vivo on neuronal migration, spine morphology, and learning and memory.** (A) Mouse Neuro-2a cells were transfected with control RNAi or RNAi specifically targeted to mouse GRK5. The samples from three independent experiments were analyzed by Western blotting and RT-PCR. ***, $P < 0.001$ (Student's *t* test). (B, left) Fluorescent images of coronal sections of P0 and P3 mouse brains in utero electroporated with control RNAi or GRK5 RNAi plasmids at E15.5. Large-scale brain images were reconstructed from images scanned by a low power lens. GFP-positive cells derived from transfected cortical progenitor cells could be visualized. Cortical layers are indicated on the right. WM, white matter. Bars, 100 μm. (right) Analysis of the distribution of transfected cortical neurons across different cortical zones at P0 and P3 from at least six sections (two per mouse) for each stage (Student's *t* test). White dotted lines indicate the margin of the cortex. (C) Genotyping of GRK5 KO mice by RT-PCR. cDNA reverse transcribed by mRNA obtained from mice were amplified by PCR using primers specially located on GRK5 exon 7 and exon 8 loci. (D) Primary hippocampal neuron cultures were dissected from WT and GRK5 KO P0 mice and electrically transfected with GFP. Cells were visualized after 24 h. Neurite number and total neurite length of 30–40 neurons from three independent cultures were analyzed. ***, $P < 0.001$ (Student's *t* test). Bar, 10 μm. (E) Cumulative probability distribution of head/neck ratios of spines ($n = 200$ from three WT and four GRK5 KO mice). GRK5 KO versus WT: 1.38 ± 0.52 versus 2.01 ± 0.77 (Kolmogorov-Smirnov test, $P < 0.01$). (F and G) Quantification of number and head/neck ratios of spines randomly selected from the dendrites ($n = 200$–250) of caudate putamen neurons from adult WT ($n = 3$) and GRK5 KO ($n = 3$) mice. (H) Cumulative probability distribution of head/neck ratios of caudate putamen neurons (Kolmogorov-Smirnov test, $P > 0.05$). (I) Locomotor test. GRK5 KO ($n = 12$); WT littermates ($n = 10$). (J and K) Open field test. GRK5 KO ($n = 12$); WT littermates ($n = 10$). (L and M) Elevated plus maze test. GRK5 KO ($n = 16$); WT littermates ($n = 20$). (N) Swim speed in Morris water maze training. GRK5 KO ($n = 22$); WT littermates ($n = 18$). (O) Escape latency to the visible platform of Morris water maze training. WT ($n = 10$) and GRK5 KO mice ($n = 12$) were subjected to visible platform water maze training for a consecutive 3 d. Error bars indicate SEM. IB, immunoblot.